

# To Explore the Effect of Preoperative Hemodynamic Factors on The Outcome of Pseudolumen After Stanford Type B Aortic Dissection TEVAR Based on Computer Fluid Dynamics

Xin He, Lulu Peng, CunWei Cheng, Fangtao Zhu, Weihua, Huang, Haibin Yu

Department of Interventional, The Second Affiliated Hospital of Zhengzhou University, Zhengzhou, China

## ABSTRACT

**Objective:** The preoperative aortic hemodynamic data of patients with Stanford type B aortic dissection were obtained by computer fluid dynamics (CFD). Then we explored the relationship between hemodynamic data and short-term residual pseudolumen after thoracic endovascular aortic repair (TEVAR) and predict the latter through the former.

**Methods:** We collected the relevant data of 53 patients who underwent TEVAR in our hospital. They were divided into the A group (residual false lumen group) and B group (closed false lumen group), according to whether there was a residual false cavity around the stent recently after TEVAR. Three-dimensional reconstruction and CFD analysis of the thoracic and abdominal aorta was performed by DSCTA before the operation to obtain the aortic wall shear stress (WSS) and maximum blood flow velocity of the true and false lumen at the entrance, middle point of the long axis, and distal decompression port at the peak time of ventricular systolic velocity. Through the statistical analysis, we further studied the predictive value of hemodynamic data for residual pseudolumen.

**Results:** There was no significant difference in age, male, preoperative and postoperative thoracic and abdominal aorta DSCTA interval, history of hypertension, history of diabetes, smoking, Pt and APTT at admission between the two groups ( $P > 0.05$ ). The blood flow velocity and shear stress at the entrance of the false lumen and the distal decompression port in the two groups were statistically significant ( $P < 0.05$ ), while the other hemodynamic indexes were not statistically significant ( $P > 0.05$ ). Binary logistic regression analysis further showed that the shear stress of the false lumen at the level of the distal decompression port (OR = 1.73,  $P = 0.01$ ) was an

independent risk factor for the residual false lumen around the stent in the early stage after TEVAR. The ROC curve analysis showed that the AUC area of the ROC curve corresponding to the shear stress of the false cavity at the level of the distal decompression port was 0.83, the best cross-sectional value was 9.49pa, and the sensitivity and specificity were 84.60% and 72.50%.

**Conclusions:** The residual pseudolumen after TEVAR is related to the hemodynamic factors in the aorta before TEVAR. Preoperative hemodynamic data also have good predictive value. When the shear stress of the false lumen at the level of the distal decompression port is greater than 9.49pa, the probability of residual false lumen around the stent during the perioperative period significantly increases.

## INTRODUCTION

Aortic dissection (AD) is an acute aortic disease with rapid progress and high mortality. If not treated in time, the mortality can reach 30%-90% [Authors/Task Force members 2014; Yangfeng 2018]. At present, clinicians often divide aortic dissection into Stanford type A and Stanford type B. And Stanford type B aortic dissection should be treated with TEVAR [Mussa 2016]. However, surgeons often only cover the proximal breach of aortic dissection. There is still a channel between the true and false cavities, so there still is a risk of rupture.

Hemodynamics is an important mechanism for the occurrence, progression, and prognosis of aortic dissection. It plays an important role in the process of false lumen thrombosis. However, it is rarely used in clinical practice because its related data are difficult to obtain [Alimohammadi 2015; Sun 2016; Bonfanti 2018]. In recent years, with the emergence of CFD, it has been used to simulate the hemodynamic parameters of AD patients. However, there is no relevant study on the prediction of the residual pseudolumen around the stent in the near future after TEVAR based on the preoperative hemodynamic data. Therefore, this study used CFD to obtain the hemodynamic data of patients with Stanford B-type ad and analyzed the relationship between the hemodynamic data and the residual pseudolumen around the stent in the near future after TEVAR, in order to effectively predict the prognosis of pseudolumen after TEVAR.

Received March 22, 2022; received in revised form June 8, 2022; accepted June 9, 2022.

Correspondence: Haibin Yu, MD, The Second Affiliated School of Zhengzhou University, Zhengzhou, China, Tel. +86 13673673661 (e-mail: 437129488@qq.com).

**DATA AND METHODS**

**General information:** We collected the relevant information from 53 patients with Stanford type B aortic dissection who underwent TEVAR in the Second Affiliated Hospital of Zhengzhou University. They were divided into group A (residual false lumen group) and group B (closed false lumen group), according to whether there was residual false lumen around the stent in the near future. There were 13 patients in group A and 40 in group B. The average age was  $50.66 \pm 10.55$  years. This study was approved by the ethics committee of the Second Affiliated Hospital of Zhengzhou University, and the subjects signed informed consent.

**Inclusion and exclusion criteria:** Inclusion criteria: Patients with Stanford type B aortic dissection; those who received TEVAR treatment and had complete CT and clinical data before and after operation; and the CT image was

clear and met the evaluation requirements. Exclusion criteria included poor image quality and patients with aortic wall ulcer [Chengzhong 2021]. According to the presence or absence of false lumen around the stent in the near future after TEVAR, the patients were divided into the A group (residual false lumen) and B group (closed false lumen).

**Image post-processing:** The preoperative CTA of the patient was reconstructed with 3D slicer software. First, the ROI (region of interest) was selected to crop the CT image of the aortic region, and then the appropriate threshold was selected to select the aorta. At the same time, the true and false cavities were divided. (Figure 2) Set the model as STL format is imported into material magics 24.0 software for further processing, and finally imported into ANSYS 16.0. First, use ICEM CFD for mesh generation. (Figure 3) Then, fluent was used for data analysis. The specific parameters and other boundary conditions were set with reference to Chen Yu [Yu 2018] and Hu Kun [Kun 2019]. After setting the aortic inlet blood flow velocity at the peak time of ventricular systole (as

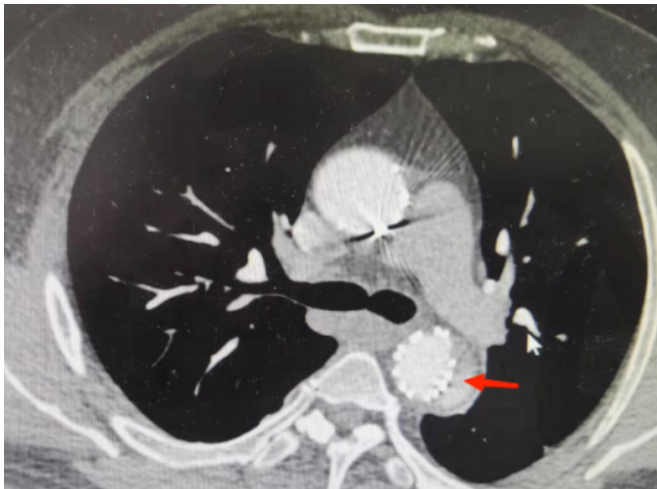


Figure 1. Short-term residual pseudolumen around stent after Stanford B aortic dissection TEVAR.

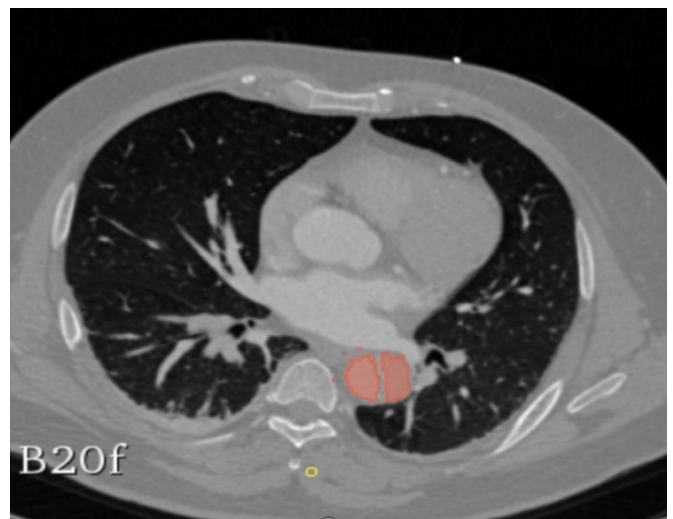


Figure 2. 3D reconstruction through 3D slicer

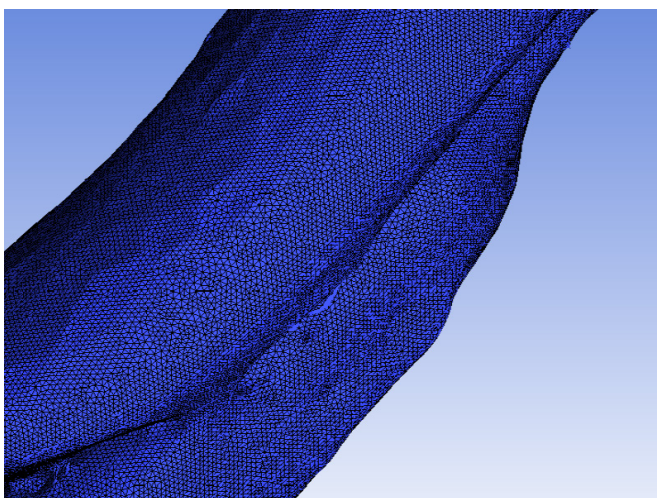


Figure 3. Grid division

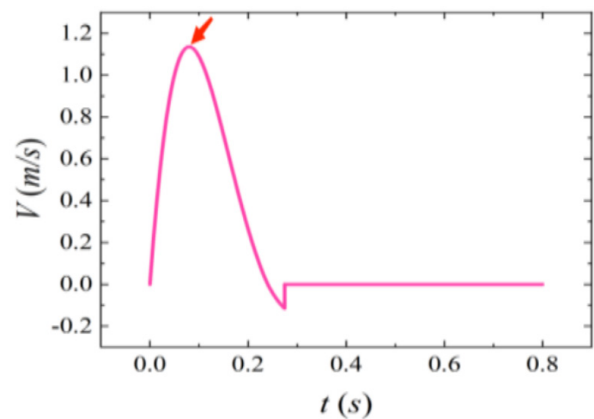


Figure 4. Aortic inlet flow velocity curve in one cardiac cycle

shown in Figure 4) for calculation, the aortic wall shear stress distribution model and blood flow velocity model were finally obtained [Yujie 2019]. (Figure 4) Take the maximum blood flow velocity and shear stress at the entrance, middle point, and distal decompression port of the true and false lumen respectively for data extraction (if there are multiple lacerations, take the nearest cardiac end as the entrance and the farthest cardiac end as the distal decompression port), as shown in Figures 5 and 6. (Figure 5) (Figure 6)

**Statistical analysis:** Spss26.0 software was used for data analysis. Normal distribution test was performed on hemodynamic data, and continuous variables conforming to normal distribution were expressed as  $(\bar{x} \pm s)$ . T-test was used for comparison between groups. The quantitative data of non-normal distribution are expressed in M (Q1, Q3), and the non-parametric test was used for the comparison between groups. The Chi-square test was used for the second category variables. The risk factors of residual false lumen around the stent were found by a binary logistic regression model. The ROC curve was used to further analyze the risk factors and evaluate the predictive efficacy of the residual pseudolumen around the stent after Stanford B aortic dissection TEVAR. The difference was statistically significant ( $P < 0.05$ ).

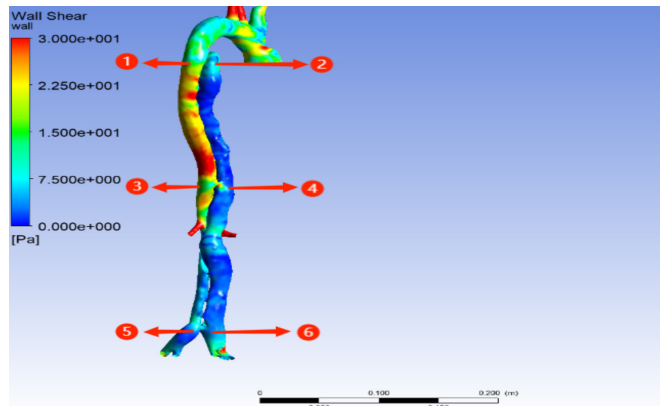


Figure 5. Shear stress of true and false cavities

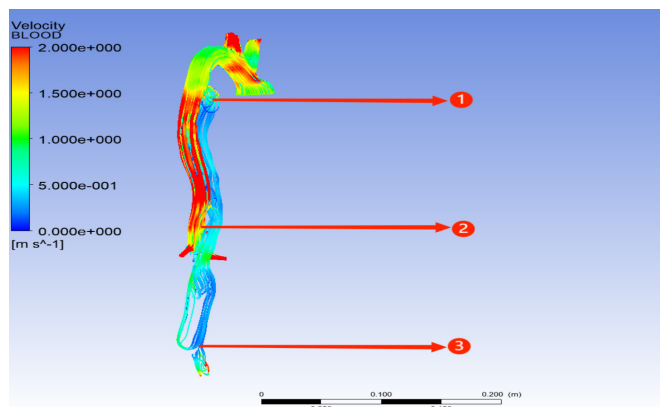


Figure 6. Blood flow diagram

## RESULTS

**Comparison of age and other data between the two groups:** There was no significant difference in age, DSCTA time interval (d), Pt and APTT between the two groups ( $P > 0.05$ ). (Table 1)

**Comparison of gender and other data the two groups:** There was no significant difference in gender, history of hypertension, history of diabetes, and smoking history between the two groups ( $P > 0.05$ ). (Table 2)

**Comparison of hemodynamic data between the two groups:** The hemodynamic data were tested for normal distribution, and the continuous variables that conformed to the normal distribution were expressed as  $(\bar{x} \pm s)$ , and a t-test was used for inter-group comparison. Quantitative data of non-normal distribution are expressed in M (Q1, Q3), and the non-parametric test was used for comparison between groups. The flow velocity and shear stress at the inlet and outlet of the false cavity in the two groups were statistically significant ( $P < 0.05$ ), while the other hydrodynamic indexes were not statistically significant ( $P > 0.05$ ). (Table 3)

The above statistically significant indicators were included in the binary logistic regression model for analysis. The shear force at the distal decompression port of the false cavity is an independent risk factor for the residual false cavity, as shown in Table 4. (Table 4) Then, the ROC curve of the shear force at the pressure reducing port at the far end of the false cavity is analyzed, as shown in Table 5, and the ROC curve is shown in Figure 7. (Table 5) (Figure 7) The AUC area of ROC curve corresponding to the shear stress at the distal decompression port of the false cavity is 0.83, the best cross-sectional value is 9.49pa, and the sensitivity and specificity are 84.60% and 72.50%.

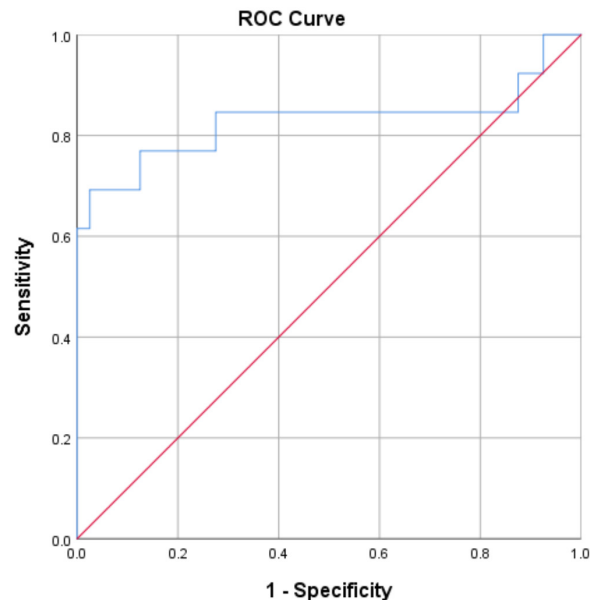


Figure 7. ROC curve of shear stress at the level of decompression port at the distal end of false cavity

Table 1. Comparison of age, DSCTA time interval (d) before and after operation between the two groups

	A group (N = 13)	B group (N = 40)	P	t
Age (y)	51.62±12.76	50.35±9.90	0.71	-0.33
CT interval days (d)	10.46±3.26	9.98±4.02	0.69	-0.40
PT (s)	15.39±5.33	14.02±1.22	0.13	-0.92
APTT (s)	40.81±7.57	41.50±23.36	0.92	0.10

Table 2. Comparison of gender and history of hypertension between the two groups

	A group (N = 13)	B group (N = 40)	P	c2
Male, n (%)	11 (84.6)	34 (85.0)	0.97	0.00
Hypertension, n (%)	8 (61.5)	31 (77.5)	0.26	1.29
Diabetes, n (%)	1 (0.20)	1 (0.03)	0.99	0.00
Smoking history, n (%)	2 (0.15)	14 (0.35)	0.32	0.98

Table 3. Comparison of hemodynamic data between the two groups

Hemodynamic data	A group (N = 13)	B group (N = 40)	P	t
Laminar velocity at the inlet of true chamber (m/s)	1.81±0.25	1.64±0.33	0.12	1.60
Layer velocity at the middle point of true chamber (m/s)	1.82±0.64	1.69±0.68	0.55	0.60
Flow velocity at the exit layer of true chamber (m/s)	1.83±1.13	2.03±0.97	0.53	-0.63
Layer velocity at inlet of false chamber (m/s)	0.72±0.32	0.54±0.25	0.03	2.19
Layer velocity at the middle point of false chamber (m/s)	0.63±0.22	0.71±0.47	0.57	-0.58
Surface velocity at the outlet of false chamber (m/s)	1.48 (1.25, 1.64)	1.04 (0.65, 1.60)	0.81	0.25
Shear stress at the entrance layer of true cavity (Pa)	15.45±5.98	12.30±5.17	0.07	1.84
Plane shear stress at the middle point of true cavity (Pa)	11.49±4.09	11.66±6.21	0.93	-0.09
Shear stress at the exit layer of true cavity (Pa)	15.65±13.94	12.13±10.33	0.33	0.98
Shear stress of false cavity inlet layer (Pa)	13.55 (6.33, 20.54)	7.39 (4.36, 10.61)	0.20	1.29
Shear stress at the middle point of false cavity (Pa)	6.62±4.38	6.34±3.28	0.81	0.25
Shear stress of false cavity outlet layer (Pa)	14.11 (10.35, 19.77)	6.31 (4.89, 9.77)	0.02	2.27

## DISCUSSION

Stanford type B aortic dissection has a lower mortality rate than type A [Yangfeng 2018]. Its pathological mechanism is very complex and involves a wide range [Simeng 2016]. In recent years, TEVAR technology has developed rapidly and is widely used in all kinds of Stanford type B aortic dissection patients. However, at present, TEVAR often only closes the proximal rupture and does not cover the distal decompression port. There is still a channel between the true cavity and the false cavity, and there is still a risk of rupture. Hemodynamics plays an important role in the occurrence, development, treatment, and prognosis of aorta. With the development of computer fluid dynamics, effective simulation of cardiovascular diseases has been

realized [Evangelista 2018; Yujie 2016; Bäumlner 2020]. The application of CFD analysis in aortic dissection model also has been realized, and its effectiveness also has been confirmed [Karmonik 2011; Papatathanasopoulou 2003; Marshall 2004; Bo 2021]. However, most of the current studies focus on the impact of TEVAR on aortic hemodynamics, and there is no research on the impact of preoperative hemodynamic data on the residual pseudolumen around the stent [Liu 2022; Dai 2018]. Therefore, this study is based on the three-dimensional reconstruction of DSCTA of preoperative patients with computer fluid dynamics and CFD processing to obtain relevant hemodynamic data. To explore whether the preoperative hemodynamic data are related to the residual pseudolumen around the stent after TEVAR, and whether the preoperative hemodynamic data can be

Table 4. Analysis of risk factors affecting prognosis after TEVAR

Risk factor	$\beta$	SE	Wald	P	OR	95% CI
Shear force at distal decompression port of pseudolumen	0.38	0.12	10.04	0.00	1.46	(1.16, 1.84)

Table 5. Predictive value of hemodynamic parameters for residual pseudolumen after TEVAR

	AUC	95% CI	Truncation value	Sensitivity (%)	Specificity (%)	P
Shear force at distal decompression port of pseudolumen	0.829	(0.65, 1.00)	9.49Pa	84.60	72.50	0.00

used to predict the residual pseudolumen around the stent after TEVAR.

In this study, the aortic inlet blood flow velocity at the peak of ventricular systolic velocity was taken as the boundary value, and the haemodynamic data were obtained by computer fluid dynamics simulation. It was confirmed that there were differences in some hemodynamic data between the residual group and closed group. The flow velocity at the entrance and shear stress at the exit of the false lumen in the two groups were statistically significant ( $P < 0.05$ ), while the other hydrodynamic parameters were not statistically significant ( $P > 0.05$ ). The blood flow velocity in the true lumen of aortic dissection often is greater than that in the false lumen, and the distal velocity tends to be greater than that in the proximal. The reason is that the configuration factors of the true and false lumen accelerate the ejection of blood flow. Therefore, the velocity of the distal decompression port is usually greater than that of the inlet [Zhao 2019]. The wall shear stress often is positively correlated with the flow velocity, so the true cavity also is larger than the false cavity. These results are similar to the research results of Chen Yu et al. [Yu 2018], which confirms the rationality of this study to a certain extent. The results of this study suggest that the flow velocity at the inlet of the false cavity in the residual group is higher than that in the closed group, suggesting that the high flow velocity at the inflow end of the false cavity is one of the important risk factors for the false cavity to be difficult to close. However, the velocity of the middle segment of the false lumen was not statistically significant ( $P > 0.05$ ). It was considered that there might be a breach between the first breach and the farthest decompression port, which might change the hemodynamic state. Binary logistic regression analysis showed that the shear force at the distal decompression port of the false lumen was an independent risk factor for the residual false lumen. The ROC curve analysis showed that the AUC area of the ROC curve corresponding to the shear stress at the distal decompression port of the false cavity was 0.83, the best cross-sectional value was 9.49pa, and the sensitivity and specificity were 84.60% and 72.50%. Therefore, when the shear stress at the distal decompression port of the false lumen is greater than 9.49pa, lipid-lowering therapy [Zhang 2012], multi-layer stacked bare stents [Resch 2006], false lumen packing [Zeng 2021] and other measures can be considered to improve the prognosis of TEVAR.

## CONCLUSIONS

The results of this study suggest that the shear stress at the level of the distal decompression port of the false lumen is a risk factor for the residual false lumen around the stent during the perioperative period after TEVAR and has a good prediction efficiency. When it is greater than 9.49pa, patients are prone to the residual false lumen around the stent during the perioperative period, thus affecting the prognosis of the false lumen after TEVAR, and measures can be taken to accelerate the thrombosis of the false lumen.

The deficiency of this study is that the sample size of this study is small, and it is a single-center retrospective study. We should continue to expand the sample size, extend the follow-up time for further confirmation, and study the multiple moments of the cardiac cycle to find the hemodynamic indexes with better prediction efficiency. And, if the model construction method and boundary conditions are different, the conclusions will be different. At present, the research in this field mostly adopts different boundary condition setting methods and model construction methods. This will bring some differences to the research conclusions in this field. If preoperative echocardiography and 4D MRI flow data are used as boundary conditions, the accuracy of conclusions will be improved.

## ACKNOWLEDGMENTS

This study was supported by Henan Provincial 2022 science and technology development project (222102310503).

## REFERENCES

- Alimohammadi M, Sherwood J M, Karimpour M, et al. 2015. Aortic dissection simulation models for clinical support: fluid-structure interaction vs. rigid wall models[J]. Biomedical engineering online. 14(1): 1-16.
- Authors/Task Force members, Erbel R, Aboyans V, et al. 2014. 2014 ESC Guidelines on the diagnosis and treatment of aortic diseases: document covering acute and chronic aortic diseases of the thoracic and abdominal aorta of the adult The Task Force for the Diagnosis and Treatment of Aortic Diseases of the European Society of Cardiology (ESC)[J]. European heart journal. 35(41): 2873-2926.

- Bäumler K, Vedula V, Sailer AM, et al. 2020. Fluid–structure interaction simulations of patient-specific aortic dissection[J]. *Biomechanics and modeling in mechanobiology*. 19(5): 1607-1628.
- Bo Y, Zhou L, Xia J, Yu S, Zhang G. 2021. Research progress on hemodynamic numerical simulation of aortic dissection[J]. *Southwest National Defense Medicine*, 2021, 31(01): 63-65.
- Bonfanti M, Balabani S, Alimohammadi M, Agu O, Homer VS, Díaz ZV. 2018. A simplified method to account for wall motion in patient-specific blood flow simulations of aortic dissection: Comparison with fluid-structure interaction[J]. *Medical engineering & physics*. 58.
- Chengzhong D, Peng X, Haodong W. 2021. The predictive value of aortic geometry on the residual false lumen around the stent in the perioperative period after endovascular repair of Stanford type B aortic dissection[J]. *Chinese Journal of Integrative Medicine, Imaging*.
- Dai Y, Dai X, Liu H. 2018. A CFD simulation study of hemodynamic changes in type B aortic dissection induced by multi-layered bare stents[C]//The 12th National Biomechanics Academic Conference and the 14th National Bioflow Compilation of abstracts of conference papers.
- Evangelista A, Isselbacher E M, Bossone E, et al. 2018. Insights from the international registry of acute aortic dissection: a 20-year experience of collaborative clinical research[J]. *Circulation*. 137(17): 1846-1860.
- Karmonik C. 2011. A Computational Fluid Dynamics Study Pre- and Post-Stent Graft Placement in an Acute Type B Aortic Dissection[J]. *Vascular and Endovascular Surgery*. 45(2).
- Kun H, editor-in-chief. 2019. ANSYS Fluent Example Detailed Explanation 1st Edition [M]. Beijing. Machinery Industry Press.
- Liu D, Zhang N, Wang W, Xu L, Liu J. 2022. Individualized hemodynamic simulation study before and after endovascular repair of Stanford type B aortic dissection[J]. *Journal of Cardiopulmonary Vascular Disease*. 41(04):404-409+417.
- Marshall I, Zhao S, Papathanasopoulou P, et al. 2004. MRI and CFD studies of pulsatile flow in healthy and stenosed carotid bifurcation models[J]. *Journal of biomechanics*. 37(5): 679-687.
- Mussa FF, Horton JD, Moridzadeh R, et al. 2016. Acute aortic dissection and intramural hematoma: a systematic review[J]. *Jama*. 316(7): 754-763.
- Papathanasopoulou P, Zhao S, Köhler U, et al. 2003. MRI measurement of time-resolved wall shear stress vectors in a carotid bifurcation model, and comparison with CFD predictions[J]. *Journal of Magnetic Resonance Imaging*. 17(2): 153-162.
- Resch TA, Delle M, Falkenberg M, Ivancev K, Konrad P, Larzon T, Lönn L, Malina M, Nyman R, Sonesson B, Thelin S. 2006. Remodeling of the thoracic aorta after stent grafting of type B dissection: a Swedish multicenter study[J]. *The Journal of cardiovascular surgery*. 47(5).
- Simeng Z, Qingsheng L, Zaiping J. 2016. Effect of aortic remodeling after endovascular repair of Stanford type B aortic dissection[J]. *Journal of Interventional Radiology*. 25(4): 302-307.
- Sun Z, Chaichana T. 2016. A systematic review of computational fluid dynamics in type B aortic dissection[J]. *International journal of cardiology*. 210: 28-31.
- Yangfeng H, Wenling Y, Wenjing F, et al. 2018. New progress in the study of the pathogenesis of aortic dissection[J]. *Advances in Cardiovascular Diseases*. 5.
- Yu C, Xin W, Yingci Z, et al. 2018. Hemodynamic analysis of Stanford type B aortic dissection based on computational fluid dynamics[J]. *Medical Biomechanics*. 6.
- Yujie S. 2019. Aortic vascular medical modeling and hemodynamic numerical simulation[D]. Inner Mongolia University for Nationalities.
- Zeng Y. 2016. Research progress in numerical simulation of Stanford type B thoracic aortic dissection[J]. *Chinese Journal of Surgery*. (006): 477-480.
- Zeng Z. 2021. An experimental study on the treatment of distal dilation after dissection with false lumen tamponade [D]. Chinese People's Liberation Army Naval Medical University.
- Zhang C, Sun Y, Li D, Zhang G, Ma R. 2012. Effects and mechanism of lipid-lowering therapy on false lumen thrombosis after aortic dissection[J]. *Shandong Medicine*. 52(06): 71-72.
- Zhao G. 2019. Research on 3D modeling and hemodynamic simulation of type B aortic dissection based on human blood vessels[D]. Guangxi University, 2019.